Modeling for Evaluation and Prediction of Effects of Short-Term Atmospheric Disturbance on Air-Sea Material Cycling

M. Fujii[1]* and A. Tanaka[2]

[1]*Faculty of Environmental Earth Science, Hokkaido University,
  N10W5, Kita-ku, Sapporo, Hokkaido 060-0810, Japan*
[2]*School of Marine Science and Technology, Tokai University,
  3-20-1, Orido, Shimizu-ku, Shizuoka, Shizuoka 424-8610, Japan*
E-mail: mfujii@ees.hokudai.ac.jp

Introduction

Both the frequency and intensity of extreme meteorological phenomena, such as storms, are predicted to be modified by global warming (IPCC 2007). Changes of meteorological parameters, such as wind speeds and precipitation, driven by changing meteorological phenomena, leads to changes of distributions of oceanic light field, temperature, salinity and nutrient concentrations, which can seriously affect the marine ecosystem and oceanic material cycling (Fig. 1). On the other hand, the atmospheric greenhouse gas (GHG) concentrations, such as CO_2, are also considered to be affected by the subsequent change of the air-sea gas exchange. Therefore, for the purpose of the sustainable use of marine biomass, and reducing atmospheric GHG concentrations, in the future, it is crucial to take steps to meet the situation based on an accurate evaluation and prediction of the effects of man-made activities, including global warming on the marine ecosystem and material cycling, and the feedback mechanism to the atmosphere. Numerical modeling is one of the useful methods for such a prediction, of which the prediction accuracy depends on the certainties of parameters embedded in the models.

However, some prognostic variables and parameters in models have large uncertainties because they have been simplified too much, or have not been calibrated sufficiently by observed results. Moreover, existing models cannot reproduce the influences of land materials discharged to the ocean through rivers on the coastal ecosystem and material cycling. Therefore, we need to implement necessary processes into models, without compromising the models' conciseness, to reduce uncertainties in the parameter values, and to improve the models' reliability for evaluating and predicting the effects of man-made activities, including global warming, on the marine ecosystem and air-sea material cycling.

Considering the current situations above, the purpose of this study was to develop a marine ecosystem model that can evaluate and predict the detailed effects of man-made activities, including global warming, on the marine biomass and bio-
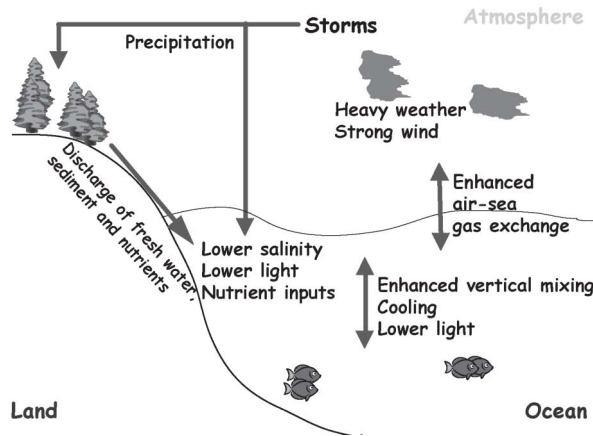
Fig. 1.   Schematic view of regions and phenomena considered in this study.

logical productivity and air-sea CO_2 exchange. In particular, this study focused on constructing a model that can reproduce realistically the effects of atmospheric disturbances such as storms, by (1) improving the air-sea CO_2 exchange process in the model, and (2) realistic parameterization of optical properties in the ocean, based on knowledge from previous observational results.

Methods

Oceanic carbon cycling

We developed a marine ecosystem model coupled with a one-dimensional physical model (Fujii *et al*. 2002, 2005, 2007b; Yamanaka *et al*. 2004; Fujii and Chai 2009). The partial pressure of CO_2 at the sea surface ($(pCO_2)_{sea}$) was calculated and the air-sea CO_2 flux can be estimated by this model. The values of biogeochemical parameters in the model are the same as those of Fujii *et al*. (2007b).

The air-sea flux of CO_2 was calculated in the model using the transfer velocity-wind speed relationships of Wanninkhof (1992) as follows:

$$\text{Air - sea } CO_2 \text{ flux}$$
$$= 0.31\, U^2 \sqrt{660 / \text{ScL}}$$
$$\cdot \left\{ \left(pCO_2\right)_{\text{sea}} - \left(pCO_2\right)_{\text{air}} \right\}, \tag{1}$$

where U is the wind speed at 10-m height (m s^{-1}), Sc is the Schmidt number for CO_2, expressed as:

$$\text{Sc} = 2073.1 - 125.62\text{SST} + 3.6276\text{SST}^2$$
$$- 0.043219\text{SST}^3, \tag{2}$$

and L is the solubility of CO_2 calculated from the temperature and salinity (Weiss 1974). The $(pCO_2)_{\text{air}}$ is the partial pressure of CO_2 in the atmosphere and the monthly in situ observational data collected in the Shemya Island, Alaska, U.S.A. (SHM; 53°N, 174°E) were used (Keeling *et al*. 1982; Conway *et al*. 1994).

The model was driven by the wind and solar radiation at the sea surface, and the temperature and salinity at the surface and at the bottom of the model domain (330-m). We used the National Centers for Environmental Prediction (NCEP) objectively-analyzed data (Kalney *et al*. 1996)

for the daily (every six hours) wind and solar radiation at the sea surface, the Reynolds weekly data for the SST (Reynolds and Smith 1995), and the KNOT (Kyodo North pacific Ocean Time-series; 44°N, 155°E) time-series observations for the temperature at the bottom, and the salinity at the surface and bottom (Fujii *et al*. 2002; Tsurushima *et al*. 2002). The model performance of reproducing the observed results were double-checked by referring to observational data obtained by the joint Japan-Canada monitoring program using ships-of-opportunity (e.g. Nojiri *et al*. 1999; Wong *et al*. 2002a, b; Zeng *et al*. 2002; Chierici *et al*. 2006).

We defined storm events as those in which the wind speed exceeded the 2σ value from a 30-day running mean. To examine the effects of storms on the biogeochemistry, we carried out two experiments: namely, Exp-1 (with storms) and Exp-2 (without storms). In Exp-1, the model was driven by the winds including those having more than 2σ values. In Exp-2, the model was driven by winds in which more than 2σ values were filtered out. The simulation was calculated from 1982 to 2000, and the 19-year monthly-mean model results were presented. See Fujii and Yamanaka (2008) for details about the experimental design.

Marine optical properties

We used a bio-optical model constructed by Fujii *et al*. (2007a). The model consists of four individual models: a physical-ecosystem model (simulating the dynamics of different ecosystem components in time and space), a photo-acclimation model (specifying the chlorophyll-to-carbon ratio of phytoplankton), an optical model (converting ecosystem state variables into inherent optical properties), and a radiative transfer model (calculating the underwater light field and the ocean color) (Fig. 2). For ease of comparison with data, we demonstrated area-averaged one-di-
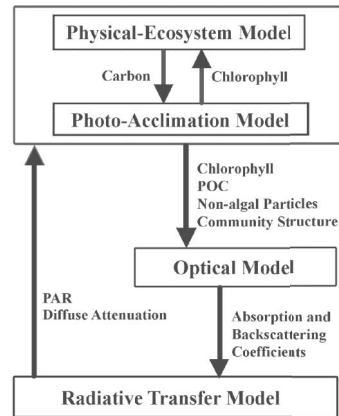

Fig. 2. Schematic view of model used in this study (modified from Fujii *et al*. 2007a).

mensional (vertical) and time-averaged results. The model, however, is formulated and designed to be used in 4 dimensions. See Fujii *et al*. (2007a) for details.

A radiative transfer model (TRAD) was also developed in this study (Tanaka 2010). The model performance was demonstrated by comparing results from both previous observations and outputs derived by another radiation transfer model of Hydrolight (Mobley *et al*. 2000a, b) used in Fujii *et al*. (2007a).

Results and Discussion

Oceanic carbon cycling

The model reproduces well the observed seasonal changes of both physical environments and biogeochemistry (Fig. 3; Fujii and Yamanaka 2008). The strong wind in winter causes the mixed layer depth (MLD), defined as the depth at which the vertical diffusive coefficient is 1.0×10^{-4} m^2 s^{-1}, to deepen dramatically to more than 100-m in late winter (Figs. 3(a) and (b)). The strong wind and pCO$_{2sea}$ elevated by storm-induced dissolved inorganic carbon (DIC) (normalized to a con-

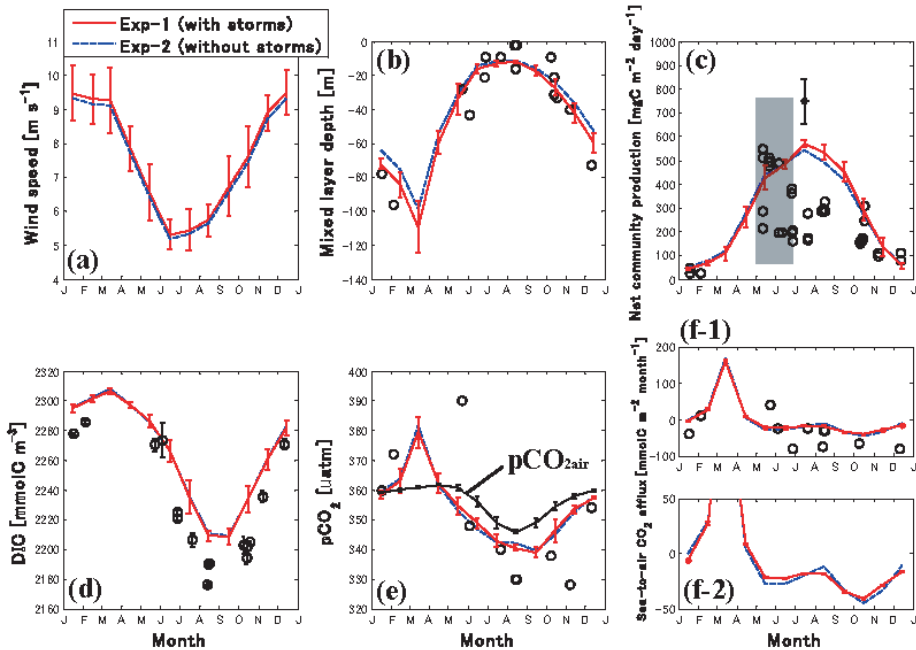**Fig. 3.** Nineteen-year (1982–2000) averaged seasonal changes of (a): wind speed [m s⁻¹], (b): MLD [m], (c): net community production [mgC m⁻² day⁻¹], (d): surface DIC [mmolC m⁻³], (e): pCO_{2sea} and pCO_{2air} [μatm], and (f-1) and (f-2): sea-to-air CO_2 flux [mmolC m⁻² day⁻¹] (positive upward), for Exp-1 (with storms; in solid red lines) and Exp-2 (without storms; in dotted blue lines) at Station KNOT (from Fujii and Yamanaka 2008). Error bars represent 1σ values. Open circles in (b), (c), (d), (e) and (f-1) denote observational data from 1998 to 2000 (from Imai *et al.* (2002) for net community production, and Tsurushima *et al.* (2002) for the others). An asterisk in (c) shows the observed net community production in July, from Shiomoto *et al.* (1998). A shaded domain in (c) denotes a range of observed net community production in May and June of 1993–1995 (from Shiomoto (2000)) but excluding data at Station 9 in 1993 which are considered to be affected by the coastal waters with extremely high net community production. Note that (f-1) and (f-2) are identical but are drawn with different *y*-axis scales.

stant salinity of 35 psu) injections into the surface waters cause tremendous sea-to-air CO_2 efflux in late winter (Figs. 3(a), (d), (e) and (f)). The net community production is low in winter because of strong light limitation on the phytoplankton growth due to the vertical dilution of the phytoplankton, along with a low irradiance in this season (Fig. 3(c)). The net community production is relatively high in spring through early autumn when the light limitation on the phytoplankton growth is alleviated by high irradiance and stratification of the surface waters in these periods.

The oceanic region functions as a sink of the atmospheric CO_2 in spring through autumn, supported by a large biological uptake of CO_2, as reported by previous observations (e.g. Tsurushima *et al.* 2002).

By comparing the model results between Exp-1 (with storms) and Exp-2 (without storms), we find that the storms contribute to the air-sea exchange of CO_2 (Fig. 3(f)). The sea-to-air CO_2 efflux is enhanced by the storms in late spring, early summer and autumn (Fig. 3(f-2)). For example, the pCO_{2sea} abruptly increased by 51 μatm during a storm passage in mid-

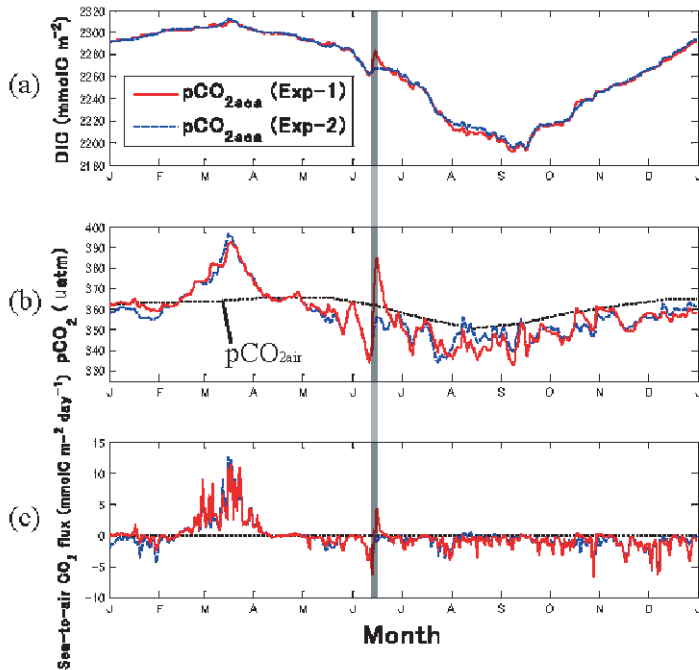**Fig. 4.** Modeled (a): surface DIC [mmolC m^{-3}], (b): pCO$_{2sea}$ and pCO$_{2air}$ [μatm], and (c): sea-to-air CO$_2$ flux [mmolC m^{-2} day^{-1}] (positive upward) for Exp-1 (with storms; in red solid lines) and Exp-2 (without storms; in blue dotted lines) in 1994 at Station KNOT (from Fujii and Yamanaka (2008)). A storm with a wind speed exceeding the 3σ value from the 30-day running mean passed during the hatched period (mid-June).

June 1994 in which the wind speed exceeded the 3σ value from the 30-day running mean (Fig. 4(b)). The pCO$_{2sea}$ reached one of its annual peaks during the storm, although the annual maximum generally appears in late winter in the subarctic western North Pacific (Fig. 3(e); Tsurushima *et al*. 2002). The sea-to-air CO$_2$ flux abruptly increased during the storm passage (Fig. 4(c)), accounting for 3% of the annual sea-to-air efflux in 1994 for two days. The sudden increase in pCO$_{2sea}$ resulted from the increase in DIC by 22 mmolC m^{-3} (Fig. 4(a)) because of the storm-induced vertical mixing, which dominated the counteracting effect of the storm-induced sea surface cooling of 0.8°C. This is consistent with a result based on data from a mooring buoy, deployed in

the East China Sea, during the passage of three typhoons in 1995 that for changes in pCO$_{2sea}$ the effect of the DIC increase dominated that of the SST decrease (Nemoto *et al*. 1999).

On the contrary, the sea-to-air efflux is reduced slightly by the storms in late summer, because the net community production is enhanced by the storm-induced nutrient injections into the surface waters (Figs. 3(c) and 3(f-2)). The model result of the decrease in the pCO$_{2sea}$ in late summer (Fig. 3(e)) is consistent with a ship-based result of Bates *et al*. (1998b), who observed a sudden decrease in pCO$_{2sea}$ in the Sargasso Sea in the subtropical gyre during the passage of hurricane Felix in August, 1995. Wanninkhof *et al*. (2007) also showed a decrease in pCO$_{2sea}$ by 12

μatm over a period of the passage of hurricane Frances in the Caribbean Sea in September, 2004. However, the cause of the storm-induced decrease in the sea-to-air CO_2 efflux is different from these studies in the subtropical regions: They observed only a slight increase in DIC, and the decrease in pCO_{2sea} was followed by a decrease in SST.

The difference in responses of pCO_{2sea} to storms between this study, and Bates *et al.* (1998b) and Wanninkhof *et al.* (2007), results from differences in the upper ocean structure and hydrographic conditions between the subarctic and subtropical gyres. In the subarctic gyre, the pycnocline is relatively shallow, and storms occasionally mix the surface waters with DIC-rich deep waters below the pycnocline. In the subtropical gyre, on the other hand, the pycnocline is usually deep, and storm-induced vertical mixing does not reach the deep waters. The magnitude of the sea surface cooling also depends on the upper ocean structure and hydrographic conditions, as noted in previous studies (e.g. Cornillon *et al.* 1987; Sakaida *et al.* 1998). Storm-induced sea surface cooling is more efficient in the subtropical ocean than in the subarctic ocean because of the permanently warm surface waters in the subtropical ocean.

The model result shows that the annual air-to-sea CO_2 influx is lower in Exp-1 (211 [mmolC m^{-2} yr^{-1}]) than in Exp-2 (218 [mmolC m^{-2} yr^{-1}]), and therefore, that the storms reduce the annual oceanic uptake of the atmospheric CO_2 efflux by 3%. It is possible that previous studies, in which the flux was calculated using the climatological wind, sea level pressure (which is necessary in converting xCO_{2air} to pCO_{2air}) and pCO_{2sea} data (e.g. Takahashi *et al.* 2002; Tsurushima *et al.* 2002), underestimated the effect of storm events on air-sea CO_2 exchange and overestimated the role of the entire subarctic western North Pacific in taking up atmos-

pheric CO_2.

Our model results also suggest that storm events, tropical or extra-tropical, could potentially have a large effect on the interannual air-sea CO_2 flux variability globally, which is consistent with Bates *et al.* (1998a) and Bates (2002). However, Wanninkhof *et al.* (2007) induced an opposite conclusion of minimal influence of storms on annual CO_2 flux. Therefore, long-term monitoring of the air-sea CO_2 flux is required in various oceanic regions to assess quantitatively the role of storm events in the interannual air-sea CO_2 flux.

The storms enhance the net community production in summer through early autumn (Fig. 3(c)), because the nutrient limitation on the phytoplankton growth is alleviated by the storm-induced nutrient injections into the surface waters. This is consistent with previous observation-based results of the oligotrophic subtropical ocean (e.g. Babin *et al.* 2004), but not as much as in the subtropical ocean, because of higher pre-storm surface nutrient concentrations and, therefore, less nutrient limitation on the phytoplankton growth, in the subarctic ocean than in the subtropical ocean. On the contrary, the storms reduce the net community production in the other seasons, because the storm-induced vertical mixing increases the light limitation on the phytoplankton growth. This result shows that the effect of storms on the phytoplankton dynamics changes with pre-storm conditions such as the irradiance and nutrient concentrations in the surface waters. The two compensating effects diminish the storm-induced annual change of the net community production at Station KNOT to only 1%.

Marine optical properties

In ecosystem models that are not coupled to an optical model, the values of biogeochemical parameters were tuned to minimize model-data misfits with vertical profiles of nutrient and chlorophyll con-

centrations and net community production in the euphotic layer (Fujii *et al.* 2007a). The vertical profile of photosynthetically active radiation (PAR) was not used to calibrate parameters in previous ecosystem models with constant light attenuation coefficients. Modeled zooplankton biomass and non-algal particle (NAP) concentration cannot be validated because very few corresponding observational data exist.

In order to examine the value of incorporating a full optical and radiative transfer model into the ecosystem model, we compared two cases, Cases 1 and 2. Case 1 uses only a rudimentary wavelength integrated model for the underwater light field (Eq. (3) below), while Case 2 is the full model using Hydrolight (Mobley *et al.* 2000a, b) to obtain the spectrally-resolved underwater light field as described in Fujii *et al.* (2007a).

The model structure in Case 1 was modified from Case 2, as follows. PAR was computed from:

$$PAR(z) \ (W \ m^{-2}) = PAR(0)$$
$$\times \exp\left\{ -k_1 z - k_2 \int_{-z}^{0} (Chl1(z) + Chl2(z))dz \right\},$$

$$(3)$$

where k_1 is the light attenuation coefficient due to water ($0.046 \ (m^{-1})$), k_2 is the light attenuation coefficient by chlorophyll ($0.048 \ (mgChl \ m^{-3})^{-1}$; e.g. Chai *et al.* 2002), and Chl1 and Chl2 is the modeled small and large phytoplankton density, respectively, in terms of chlorophyll ($mgChl \ m^{-3}$).

In Case 1, the light attenuation coefficients were set to the same as in Chai *et al.* (2002) (Fujii *et al.* 2007a). In this case, as in most previous ecosystem modeling studies, observed PAR values and associated decreases with depth are not referred to in tuning the model parameters. Therefore, the parameters were tuned to mini-

mize model-data misfits with vertical profiles of nutrient and chlorophyll concentrations and net community production, which requires modification of the zooplankton maximum specific grazing rate from Case 2. The model results show similar vertical profiles of $Si(OH)_4$ concentration and net community production, relatively low surface NO_3 concentration, and a higher and deeper chlorophyll maximum, compared with those in Case 2, although the results of both models were within the observations.

Phytoplankton community assemblage can also be reproduced by the model with optics (Case 2). In Chai *et al.* (2002), using the non-spectrally-resolved ecosystem model, they tuned the water-column phytoplankton assemblage so that the percentage of diatoms to the total phytoplankton biomass is nearly 16%, referring to the observed ranges from 5% to 20% (Bidigare and Ondrusek 1996). With the spectrally-resolved bio-optical model (Case 2), we could tune the vertical phytoplankton assemblage more accurately, referring to not only measurements of each phytoplankton biomass but also those of the contribution of diatoms to the total phytoplankton derived from optical properties (absorption and backscattering).

These results suggest that both ecosystem model results, with or without optics, can reproduce the observed fundamental biogeochemical properties, as long as the correct diffuse light attenuation is used. Since the PAR data are not consistent with the simple chlorophyll formulation used in previous studies (e.g. Chai *et al.* 2002), another source of diffuse light attenuation is needed for the model that can take into account contributions by NAP and colored dissolved organic matter (CDOM). Our bio-optical model provided such a value (Fig. 5).

In addition, the coupled model results illustrate its capability to be constrained using observations of optical variables and,
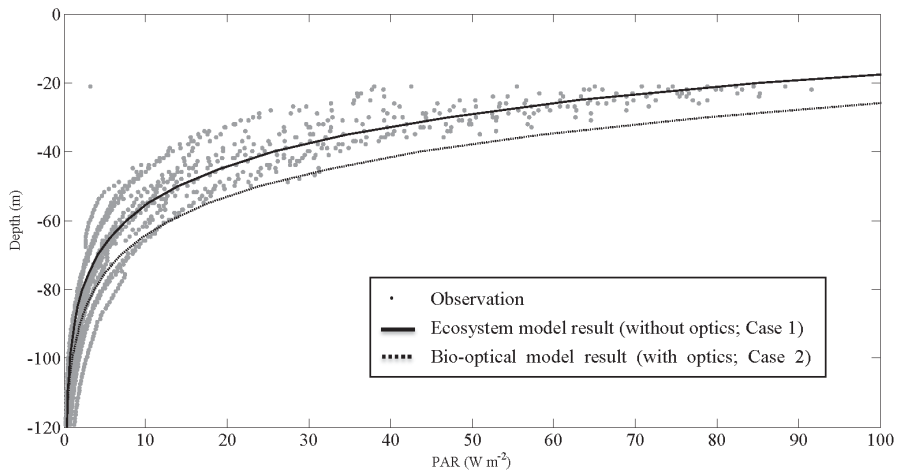
Fig. 5. Vertical profile of PAR (W m^{-2}) simulated by an ecosystem model (without optics; Case 1) and a bio-optical model (with optics; Case 2). Dots denote the U.S. JGOFS EqPac observations in August–September (Survey II; TT011) and October (Time series II; TT012) of 1992 (Murray *et al.* 1995; Barber *et al.* 1996).

thus, its ability in improving model performance, which currently cannot be done with available biological properties alone. Additional constituents, which should be added to future ecosystem models, such as DOM, bacteria, and coccoliths (e.g. Fujii and Chai 2007), are likely to improve the optics-simulation model fit assuming the relevant data on their abundance can be obtained.

While we were able to reproduce most of the observations by simply changing the diffuse attenuation values in the model lacking optics (Case 1), this approach is not likely to work in temporally-varying simulations where the diffuse attenuation coefficient changes in time; any changes in the relative proportion of the biogeochemical variables contributing to absorption (and to a lesser degree to backscattering) would result in changes in the diffuse attenuation parameters in Eq. (3). Simulating these changes requires having the appropriate biogeochemical constituents and related optical properties, most of which are captured by the bio-op-

tical model (with the important exception of CDOM).

Radiative transfer model

A radiative transfer model (TRAD) was newly developed in this study (Tanaka 2010; Tanaka *et al.* 2011). In this model, the vertical and angular distributions of underwater radiance were computed without using an empirical procedure, by assuming that a water body comprises numerous parallel horizontal layers. The model was validated using the observation data obtained from Lake Pend Oreille and Suruga Bay, and for highly scattering water.

Although TRAD consists of simple equations of which physical interpretation is easy, the results obtained with TRAD are in good agreement with the observational data and outputs obtained by Hydrolight (Tanaka 2010). As the layer thickness is quantitatively evaluated in TRAD with the help of the error estimator, the model can predict underwater light fields with sufficient accuracy for various
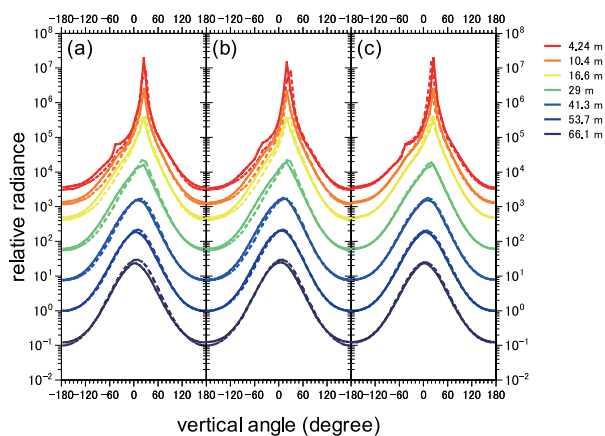
Fig. 6. The computed and observed radiance distribution in the plane of the sun (from Tanaka (2010)). (a) solid line: TRAD, dashed line: Lake Pend Oreille (b) solid line: HydroLight, dashed line: Lake Pend Oreille (c) solid line: TRAD, dashed line: HydroLight.

oceanic conditions. In addition, since its physical interpretation is simple, TRAD can be applied to a wide range of oceanographic problems. TRAD will be a useful tool for developing an algorithm for ocean color remote sensing.

The availability of an equation to show the exact influence of multiple scattering in the single scattering process (Tanaka *et al*. 2011). The derived equation was effective in estimating the computational radiance error, owing to the discretization of the optical depth by TRAD, that is the successive order of scattering method. It also provided a theoretical background for estimating the computational error, and can be applied to other numerical models.

Conclusions

We have developed an ecosystem model, and examined the biogeochemical responses to storms. In the simulation, the storms affect both the ecosystem dynamics and the air-sea CO_2 exchange, and the effects change with the upper ocean structure and hydrographic conditions. The storms enhance the net community production in summer through early autumn be-

cause of the storm-induced nutrient injections into the surface waters. On the contrary, the net community production in the other seasons is reduced by the storm-driven vertical mixing and subsequent intention of the light limitation on the phytoplankton growth. The two compensating effects diminish the storm-induced annual change of net community production to only 1%. The storms enhance the sea-to-air CO_2 efflux in late spring, early summer and autumn by the strong wind, whereas the storms reduce the sea-to-air CO_2 efflux in late summer because of a large biological uptake of CO_2 stimulated by the storm-induced nutrient injections into the surface waters. The storms are estimated to reduce the annual oceanic uptake of the atmospheric CO_2 flux by 3% in this region. During storms, pCO_{2sea} tends to increase more in the subarctic ocean because of the storm-induced increase in surface DIC, whereas pCO_{2sea} tends to decrease in the subtropical ocean because of the storm-induced decrease in the SST. Therefore, it is necessary to perform direct measurements during storm passage in various oceanic regions to elucidate which effects dominate the storm-induced

pCO_{2sea} change in each region. Previous studies that calculated the air-sea CO_2 flux using climatological wind, sea level pressure and pCO_2 data probably underestimated the contribution of storms to the air-sea CO_2 exchange. Therefore, to reduce uncertainties in the global oceanic CO_2 uptake, changes in these parameters caused by episodic atmospheric disturbances should be measured continuously. While climate changes associated with global warming may influence the frequency and intensity of storms (e.g. Emanuel 1987, 2005; Beersma *et al.* 1997; Saunders and Harris 1997; Sugi *et al.* 2002; Geng and Sugi 2003; Yoshimura and Sugi 2005; Webster *et al.* 2005; Yoshimura *et al.* 2006), storm-induced biogeochemical activity may also contribute to climate. Therefore, to predict future climate change, it is essential that we elucidate the biogeochemical responses to storms. Although it is difficult to conduct direct observations during rough weather, we would very much like to have high-frequency, in-situ biogeochemical observations with which we could conduct more accurate simulations.

We also developed an ecosystem model that explicitly represents biogeochemically and optically. We found that utilizing an optical model to convert from ecosystem model state variables to optical parameters, and a realistic subsurface light, provides:

(1) more data to compare model output by providing a more rigorous test of model formulation and choice of parameter values, especially for those that are difficult to measure with high resolution in time and space, (2) the required input to obtain a realistic subsurface light field by linking the optics to a radiative-transfer model (Hydrolight), and (3) improved simulation realism with respect to key biogeochemical processes, such as photosynthesis, which are crucial for assessing oceanic carbon cycling and food web dynamics. The additional optical measurements, being routinely available from research vessels, autonomous platforms, and space-borne observations, can now be used directly for comparison and testing of the output of our new coupled bio-optical model. This is an improvement over the limited number of variables that can be used to test our previous ecosystem models with no explicit optical properties. Incorporating radiative transfer models, such as TRAD developed in this study, to ecosystem models, would also contribute to improving the realistic simulations of physical-bio-optical interactions, although these capabilities were not tested here.

Acknowledgements

References

Babin SM, Caton JA, Dickey TD, Wiggert JD (2004) Satellite evidence of hurricane-induced phytoplankton blooms in an ocean desert. J. Geophys. Res. **109**: C03043, doi:10.1029/2003JC001938.

Barber RT, Sanderson MP, Lindley ST, Chai F, Newton J, Trees CC, Foley DG, Chavez FP (1996) Primary productivity and its regulation in the equatorial Pacific during and following the 1991–1992 El Niño. Deep-Sea Res. Part II **43**(4–6): 933–969.

Bates NR (2002) Interannual variability in the global uptake of CO_2. Geophys. Res. Lett. **29**(5): doi:10.1029/2001GL013571.

Bates NR, Knap AH, Michaels AF (1998a) Contribution of hurricanes to local and global estimates of air-sea exchange of CO_2. Nature **395**: 58–61.

Bates NR, Takahashi T, Chipman DW, Knap AH (1998b) Variability of pCO_2 on diel to seasonal timescales in the Sargasso Sea near Bermuda. J. Geophys. Res. **103**: 15567–15585.

Beersma JJ, Rider KM, Komen GJ, Kaas E, Kharin VV (1997) An analysis of extra-tropical storms in the

North Atlantic region as simulated in a control and $2 \times CO_2$ time-slice experiment with a high-resolution atmospheric model. Tellus A **49**(3): 347–361.

Bidigare RR, Ondrusek ME (1996) Spatial and temporal variability of phytoplankton pigment distributions in the central equatorial Pacific Ocean. Deep-Sea Res. Part II **43**(4–6): 809–833.

Chai F, Dugdale RC, Peng T-H, Wilkerson FP, Barber RT (2002) One-dimensional ecosystem model of the equatorial Pacific upwelling system. Part I: model development and silicon and nitrogen cycle. Deep-Sea Res. Part II **49**: 2713–2745.

Chierici M, Fransson A, Nojiri Y (2006) Biogeochemical processes as drivers of surface fCO_2 in contrasting provinces in the subarctic North Pacific Ocean. Global Biogeochem. Cycles **20**: GB1009, doi:1029/2004GB002356.

Conway TJ, Masarie KA, Zhang N (1994) Evidence for interannual variability of the carbon cycle from the National Oceanic and Atmospheric Administration/Climate Monitoring and Diagnostics Laboratory Global Air Sampling Network. J. Geophys. Res. **99**(D11): 22831–22855.

Cornillon P, Stramma L, Price JF (1987) Satellite measurements of sea surface cooling during hurricane Gloria. Nature **326**: 373–375.

Emanuel KA (1987) The dependence of hurricane intensity on climate. Nature **326**: 483–485.

Emanuel K (2005) Increasing destructiveness of tropical cyclones over the past 30 years. Nature **436**: 686–688, doi:10:1038/nature03906.

Fujii M, Chai F (2007) Modeling carbon and silicon cycling in the equatorial Pacific. Deep-Sea Res. Part II, doi:10.1016/j.dsr2.2006.12.005.

Fujii M, Chai F (2009) Influences of initial plankton biomass and mixed-layer depths on the outcome of iron-fertilization experiments. Deep-Sea Res. Part II **56**: 2936–2947.

Fujii M, Yamanaka Y (2008) Effects of storms on primary productivity and air-sea CO_2 exchange in the subarctic western North Pacific: a modeling study. Biogeosciences **5**: 1189–1197.

Fujii M, Nojiri Y, Yamanaka Y, Kishi MJ (2002) A one-dimensional ecosystem model applied to time series station KNOT. Deep-Sea Res. Part II **49**: 5441–5461.

Fujii M, Yoshie N, Yamanaka Y, Chai F (2005) Simulated biogeochemical responses to iron enrichments in three high nutrient, low chlorophyll (HNLC) regions. Prog. Oceanogr. **64**: 307–324, doi:10.1016/j.pocean.2005.02.017.

Fujii M, Boss E, Chai F (2007a) The value of adding optics to ecosystem models: a case study. Biogeosciences **4**: 817–835.

Fujii M, Yamanaka Y, Nojiri Y, Kishi MJ, Chai F (2007b) Comparison of seasonal characteristics in biogeochemistry among the subarctic North Pacific stations described with a NEMURO-based marine ecosystem model. Ecol. Model. **202**: 52–67.

Geng Q-Z, Sugi M (2003) Possible change of extratropical cyclone activity due to enhanced greenhouse gases and sulfate aerosols.—Study with a high-resolution AGCM. J. Climate **16**: 2262–2274.

Imai K, Nojiri Y, Tsurushima N, Saino T (2002) Time series of seasonal variation of primary productivity at station KNOT (44°N, 155°E) in the sub-arctic western North Pacific. Deep-Sea Res. Part II **49**: 5395–5408.

IPCC (2007) *Climate Change 2007. The Physical Science Basis. Contribution of Working Group I to the Fourth Assessment Report of the Intergovernmental Panel on Climate Change*. Cambridge University Press, 996 pp.

Kalney E, Kanamitsu M, Kistler R, Collins W, Deaven D, Gandin L, Iredell M, Saha S, White G, Woollen J, Zhu Y, Chelliah M, Ebisuzaki W, Higgins W, Janowiak J, Mo KC, Ropelewski C, Wang J, Leetmaa A, Reynolds R, Jenne R, Joseph D (1996) The NCEP/NCAR 40-year reanalysis project. Bull. Am. Meteorol. Soc. **77**: 437–471.

Keeling CD, Bacastow RB, Whorf TP (1982) Measurements of the concentration of carbon dioxide at Mauna Loa Observatory, Hawaii. *Carbon Dioxide Review: 1982* (ed. Clark WC), Oxford University Press, New York.

Mobley CD, Sundman LK (2000a) Hydrolight 4.1 User's Guide. Sequoia Scientific, Inc., Redmond, Washington, D.C.

Mobley CD, Sundman LK (2000b) Hydrolight 4.1 Technical Documentation. Sequoia Scientific, Inc., Redmond, Washington, D.C.

Murray JW, Johnson E, Garside C (1995) A US JGOFS process study in the equatorial Pacific (EqPac): Introduction. Deep-Sea Res. Part II **42**(2–3): 275–293.

Nemoto K, Takatani S, Ogawa K, Umeda T, Oyama J, Midorikawa T, Kimoto T, Inoue HY (1999) Continuous observations of atmospheric and oceanic CO_2 using the moored buoy in the East China Sea. *Proceedings of the 2nd International Symposium CO_2 in the Oceans*, CGER/NIES, Tsukuba, pp.

545–553.

Nojiri Y, Fujinuma Y, Zeng J, Wong CS (1999) Monitoring of pCO_2 with complete seasonal coverage utilizing a cargo ship M/S Skaugran between Japan and Canada/US. *Proceedings of the 2nd International Symposium CO_2 in the Oceans*, CGER/NIES, Tsukuba, pp. 17–23.

Reynolds RW, Smith TM (1995) A high resolution global sea surface temperature climatology, J. Climate **8**: 1571–1583.

Sakaida F, Kawamura H, Toba Y (1998) Sea surface cooling caused by typhoons in the Tohoku Area in August 1989. J. Geophys. Res. **103**: 1053–1065.

Saunders MA, Harris AR (1997) Statistical evidence links exceptional 1995 Atlantic hurricane season to record sea warming. Geophys. Res. Lett. **24**: 1255–1258.

Shiomoto A (2000) Chlorophyll-a and net community production during spring in the oceanic region of the Oyashio Water, the north-western Pacific. J. Mar. Biol. Ass. U.K. **80**: 343–354.

Shiomoto A, Ishida Y, Tamaki M, Yamanaka Y (1998) Net community production and chlorophyll a in the western Pacific Ocean in summer. J. Geophys. Res. **103**(C11): 24651–24661.

Sugi M, Noda A, Sato N, (2002) Influence of the global warming on tropical cyclone climatology: an experiment with the JMA global model. J. Meteorol. Soc. Jpn. **80**: 249–272.

Takahashi T, Sutherland SC, Sweeney C, Poisson A, Metzl N, Tilbrook B, Bates N, Wanninkhof R, Feely RA, Sabine C, Olafsson J, Nojiri Y (2002) Global sea-air CO_2 flux based on climatological surface ocean pCO_2, and seasonal biological and temperature effects. Deep-Sea Res. Part II **49**: 1601–1622.

Tanaka A (2010) Numerical model based on successive order of scattering method for computing radiance distribution of underwater light fields. Optics Express **18**: 10127–10136.

Tanaka A, Fujii M, Oishi T (2011) Availability of an equation to evaluate error by optical path discretization in radiative transfer computation based on the successive order of scattering method. J. Oceanogr. **68**(1): 215–218, doi:10.1007/s10872-011-0087-3.

Tsurushima N, Nojiri Y, Imai K, Watanabe S (2002) Seasonal variations of carbon dioxide system and nutrients in the surface mixed layer at station KNOT (44°N, 155°E) in the subarctic western North Pacific. Deep-Sea Res. Part II **49**: 5377–5394.

Wanninkhof R (1992) Relationship between wind speed and gas exchange. J. Geophys. Res. **97**(C5): 7373–7382.

Wanninkhof R, Olsen A, Trinanes J (2007) Air-sea CO_2 fluxes in the Caribbean Sea from 2002–2004. J. Mar. Syst. **66**: 272–284.

Webster PJ, Holland GJ, Curry JA, Chang H-R (2005) Changes in tropical cyclone number, duration, and intensity in a warming environment. Science **309**: 1844–1846.

Weiss RF (1974) Carbon dioxide in water and seawater: The solubility of a non-ideal gas. Mar. Chem. **2**: 203–215.

Wong CS, Waser NAD, Nojiri Y, Johnson WK, Whitney FA, Page JSC, Zeng J (2002a) Seasonal and interannual variability in the distribution of surface nutrients and dissolved inorganic carbon in the Northern North Pacific: Influence of El Niño. J. Oceanogr. **58**: 227–243.

Wong CS, Waser NAD, Nojiri Y, Whitney FA, Page JS, Zeng J (2002b) Seasonal cycles of nutrients and dissolved inorganic carbon at high and mid latitudes in the North Pacific Ocean during the Skaugran cruises: determination of new production and nutrient uptake ratios. Deep-Sea Res. Part II **49**: 5317–5338.

Yamanaka Y, Yoshie N, Fujii M, Aita MN, Kishi MJ (2004) An ecosystem model coupled with Nitrogen-Silicon-Carbon cycles applied to Station A7 in the Northwestern Pacific. J. Oceanogr. **60**: 227–241.

Yoshimura J, Sugi M (2005) Tropical cyclone climatology in a high-resolution AGCM—Impact of SST warming and CO_2 increase—. SOLA **1**: 133–136.

Yoshimura J, Sugi M, Noda A (2006) Influence of global warming on tropical cyclone frequency. J. Meteor. Soc. Japan **84**: 405–428.

Zeng J, Nojiri Y, Murphy PP, Wong CS, Fujinuma Y (2002) A comparison of ΔpCO_2 distributions in the northern North Pacific using results from a commercial vessel in 1995–1999. Deep-Sea Res. Part II **49**: 5303–5315.